Integrative and Comparative Biology

Integrative and Comparative Biology, volume 0, number 0, pp. 1–9
https://doi.org/10.1093/icb/icab123

Society for Integrative and Comparative Biology

SYMPOSIUM

Morphogenesis of Iridescent Feathers in Anna's Hummingbird *Calypte anna*

Liliana D'Alba[*,1], Melissa Meadows[†], Rafael Maia[‡], Jong-Souk Yeo[§], Marie Manceau[¶] and Matthew D. Shawkey[*]

[*]Evolution and Optics of Nanostructures Group, Department of Biology, University of Ghent, Ledeganckstraat 35, Ghent 9000, Belgium; [†]Department of Biology, University of Florida, 220 Bartram Hall, Gainesville, FL 32611-8525, USA; [‡]Department of Ecology, Evolution and Environmental Biology, Columbia University, New York, NY 10027, USA; [§]School of Integrated Technology, Yonsei University, Incheon 21983, Republic of Korea; [¶]Center for Interdisciplinary Research in Biology, CNRS 7241, INSERM U1050, Collège de France, Paris 75231, France

From the symposium "The Integrative Biology of Pigment Organelles" presented at the annual meeting of the Society for Integrative and Comparative Biology virtual annual meeting, January 3–February 28, 2021.

[1]E-mail: liliana.dalba@ugent.be

Synopsis Color is a phenotypic trait of utmost importance, particularly in birds, which are known for their diverse color signals and color-producing mechanisms including pigment-based colors, light scattering from nanostructured feather tissues and combinations thereof. Bright iridescent plumage colors of hummingbirds are caused by light scattering by an organized array of flattened, pigment organelles, containing air-filled vesicles, called melanosomes. These hollow platelets are organized in multilayer arrays that contain numerous sharp air/melanin refractive index interfaces, producing brilliant iridescent colors. Despite their ecological significance and potential for inspiration of new optical materials, how platelets form and spatially arrange in nanostructures in growing feathers remains unknown. Here, we tested the hypothesis that melanosome formation and organization occurs mostly through passive self-assembly processes by assembling a developmental time series of growing hummingbird feathers using optical and electron microscopy. We show that hummingbird platelets contain air bubbles or vesicles upon their formation in pigment-producing cells, melanocytes. When melanosomes are transferred to neighboring keratinocytes (the cells shaping barbule structure) they drastically expand in size; and variation in this enlargement appears to be driven by physical constraints caused by the placement of the melanosomes within the barbule plate and their proximity to other melanosomes. As the barbule elongates and narrows, polymerizing feather corneous beta-protein orients melanosomes unilaterally, forcing them into a stacked configuration. These results reveal potentially novel forces driving the self-assembly of the nanostructures producing some of the brightest colors in nature.

Introduction

Colors have critical functions both in the manmade and natural worlds, ranging from camouflage to communication to thermoregulation (Cott and Huxley1940). Different colors are produced by different mechanisms. Black, brown, and gray colors are produced by the melanin pigment, which possesses broadband light absorption properties across the visible spectrum (Hill and McGraw 2006). Other pigments like carotenoids and pterins selectively absorb wavelengths to produce highly saturated colors (Hill and McGraw 2006), but these are largely limited to yellows and reds and only rarely produce shorter wavelength hues (e.g., blues and violets). By contrast, structural colors resulting from coherent scattering of light by highly ordered nanostructures span most of the visible spectrum (Srinavasarao 1999; Prum 2006), and, unlike pigment-based colors, can produce iridescent effects. The production of highly reflective, iridescent colors depends on a combination of nanoscale organization of feather components, high refractive index (RI) contrast between feather corneous beta-protein (CβP; Alibardi 2016), melanin, and/or air

Advance Access publication June 9, 2021

(Prum 2006). Feather nanostructures can be organized in one (e.g., multilayer reflectors), two (e.g., 2D photonic crystals), or three dimensions (e.g., amorphous matrices) (Prum 2006).

Counter-intuitively, some of the brightest colors in nature are produced by nanoscale arrangements of the dark, melanin-containing organelles called melanosomes (Maia et al. 2013; Eliason et al. 2013). Melanin strongly absorbs light, but also has a high RI (estimates range from ~1.7 to 2.0, Xiao et al. 2020) that can sharply contrast with those of other materials with lower RI such as feather CβP (~1.56) and, in particular, air (1.0). Thus, when melanin is spatially arranged with CβP or air, it can produce bright iridescent colors. In the absence of spatial organization, these melanosomes produce typical dark melanin-based colors.

Optical nanostructures enable the production of colors otherwise difficult to produce, for example, green colors that require rare pigments (Durrer 1986). In turn, the functions enabled by these colors such as camouflage may have enabled colonization of new niches or generation of new colors for sexual selection (Maia et al. 2013). The ability of nanostructures to selectively interact with wavelengths of light with high precision, and to be "tuned" to certain wavelengths through slight changes in dimensionality makes them ideal inspirations for novel optical devices, fibers and coatings (Parker and Townley 2007).

Despite the significance of structural colors to both biology and engineering, how they form in developing tissues remains largely unknown. For birds, this holds true for both the development of modified (hollow and/or flattened) melanosomes and the nanostructures they comprise. Shawkey et al. (2015) suggested that hollow cylindrical melanosomes in feathers of the wild turkey (*Meleagris gallopavo)* result from selective loss of pheomelanin cores following their deposition in developing barbules. By contrast, Durrer and Villiger (1967) suggested that hollow, flattened melanosomes in the lesser blue-eared glossy starling *(Lamprotornis chloropterus*) form by deposition of melanin on air bubbles in pre-melanosomes within the melanocyte itself. Their high degree of organization suggests some level of active cellular control through, for example, microfibrils, but thus far, theoretical and empirical studies on this topic have been limited either to a few feathers with a simple bilayer film (Durrer and Villiger 1967; Maia et al. 2012; Rubenstein et al. 2021) or hexagonal lattice of melanin and feather CβP (Shawkey et al. 2015), a quasi-ordered structure of CβP and air (Dufresne et al. 2009) or a multilayer structure in a leaf beetle (Onelli et al. 2017). These studies suggest that in fact, optical nanostructures form through self-assembly processes with little active cellular input other than the specification of initial conditions for self-assembly.

Whether these passive patterns of development are conserved across species is unknown. Hummingbirds produce highly reflective and strongly iridescent colors through their unique nanostructural arrays of air-filled platelet-shaped melanosomes (Greenewalt et al. 1960; Eliason et al. 2020; Fig. 1). These platelet arrays appear to function as multilayer reflectors in conjunction with a thin outer cortex layer surrounding, in some species a layer of smaller melanosomes (this study). Iridescence is enhanced by flat upper surfaces and boomerang-shaped barbules, which causes dramatic color shifts with changes in angle of viewing (Giraldo et al. 2018). Here, we examine patterns of development in iridescent gorget feathers of Anna's hummingbirds (*Calypte anna*), using light and electron microscopy to test the hypothesis that melanosomes organize through passive processes of self-assembly. In particular, we studied (1) the growth of hollow platelet-shaped melanosomes, (2) their organization at the nanoscale, and (3) the ontogenetic changes in barbule shape. We show that these three processes are interconnected and indeed our results show that changes in one can profoundly affect the others. Furthermore, our results suggest that some previously unconsidered physical processes, such as foaming, play critical roles in nanostructure growth.

Methods

Sample collection and preparation

We used 10 developing feather germs (pin feathers), plucked as part of a previous study (see detailed methods in Meadows et al. 2012). Briefly, using forceps, we carefully plucked one pin feather (encased in their sheath) from the gorget of 10 individual Anna's hummingbirds (*C. anna*). Growing feathers were collected 6 days after moult and had an average length of 14 mm.

Developing pin feathers present a proximo-distal gradient of maturation, where young cells proliferate basally and older keratinocytes are displaced upward (Prum 1999; Fig. 1). Thus, distal cells are older and more mature than proximal cells and by cutting successive sections along this gradient from a single feather we can construct a time series of melanosome and barbule development (Alibardi 2007; Prum et al. 2009, Maia et al. 2012; Shawkey et al. 2015).

We fixed pin feathers overnight in 4% glutaraldehyde in 0.1 M phosphate buffer solution, then rinsed them in phosphate buffer and post-fixed them in 2% OsO_4 in buffer for 90 min. After rinsing them three times in distilled water, we dehydrated and infiltrated them with increasing concentrations (15%, 50%, 70%, and 100%) of epoxy resin (EMbed-812; Electron Microscopy

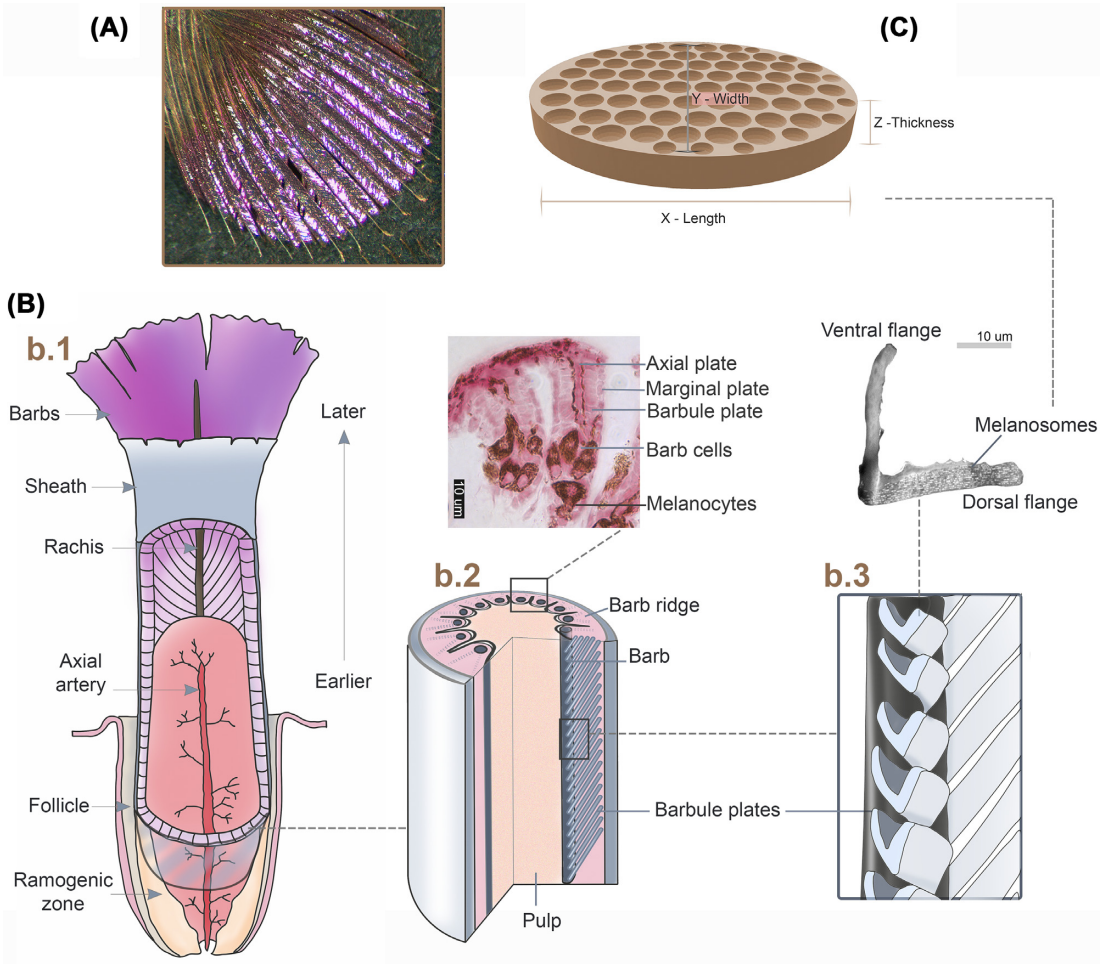

Fig. 1 Overview of feather morphology and growth of *Calypte anna hummingbird* feathers. (**A**) Photograph of a mature iridescent gorget feather. (**B**) b.1: Schematic drawing illustrating the main structural components of a pin feather and denoting a proximo-distal gradient in feather cell maturation. b.2: Germinal collar of the pin feather showing the location of barb ridges, inside which the developing barb and barbule cells are located, the inset shows an optical micrograph detailing the cellular components of barb ridges in cross-section. b.3: Illustration of a slice along the barb axis, where proximal barbules, cross-sectioned, show their typical boomerang shape; the inset shows an electron micrograph of a mature barbule in cross-section where the aligned rows of melanosomes are shown inside the dorsal flange of the barbule. (**C**) Schematic 3D illustration of a typical elliptical hummingbird melanosome containing numerous holes or vesicles. Axes measured in the study are shown. Scale bars: b.2 and b.3 micrographs 10 μm. b.1 modified after Foth 2020. b.2 modified after Watterson (1942). Illustrations by L. D'Alba.

Sciences, PA, USA) followed by 16-h polymerization in epoxy resin at 60°C in a laboratory oven.

Histology and microscopy

To visualize melanosome and barbule developmental trajectories, we cut thick longitudinal sections for light microscopy (thickness = 2 μm) and for transmission electron microscopy (thickness = 100 nm) from entire pin feathers. Thus, these longitudinal sections span from the follicle base to its tip (i.e., from the least- to most-developed regions). Thick sections were placed on glass slides and thin sections were collected using oval-slit carbon and formvar-coated copper grids in duplicate, and stained with Uranyless/lead citrate (D'Alba et al. 2019). Briefly, we inserted grids containing samples in a staining matrix (Electron Microscopy Sciences, PA, USA) and stained them by pipetting 9 ml of Uranyless (Electron Microscopy Sciences, PA, USA) into the vessel containing the matrix. After 2 min we rinsed the matrix five times using distilled water, followed by a bath of lead citrate for 2 min and 5 water rinses. We observed thick sections on an optical microscope (Leica DM 1000), and thin sections on a JEOL JEM 1010 (Jeol Ltd, Tokyo, Japan) transmission electron microscope operating at 120 kV.

Results

Barbule maturation

We identified four phases of barbule maturation. In phase 1 (P1; Fig. 2B), barbule cells at the base of the

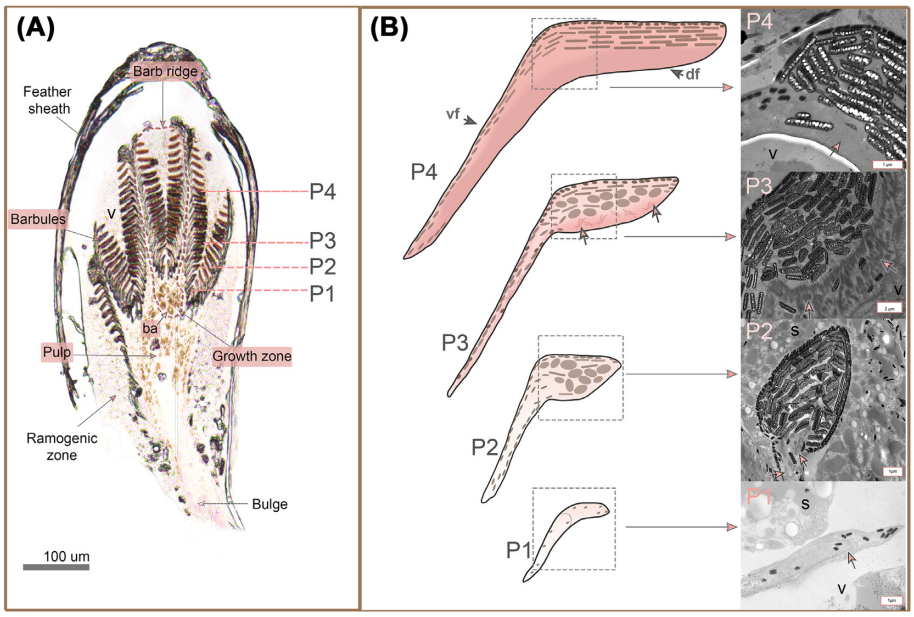

Fig. 2 Ontogenetic changes in hummingbird barbules. (**A**) Longitudinal section of a developing gorget feather encased in its sheath. (**B**) Phases of barbule maturation: Phase one (P1) is observed within barb ridges within the ramogenic zone (the zone of cell proliferation: 0 nm distance), two separate cells of the barbule cell chain (arrow) are seen surrounded by supportive cells (s). In phase two (P2 ~100 nm distance), the apical cytoplasm in cells swells giving them a rounder shape, a fold in these cells appears, forming the two barbule flanges. Few electron-dense corneous beta-bundles emerge (pink arrows). In phase 3 (P3; ~250 nm), corneous beta-bundles (arrows) are numerous on the lower side of the barbule cell. In phase 4 (P4; >300 nm), melanosomes are fully aligned on the upper side of the cell on the dorsal flange (df), and concentrated around the edges of the ventral flange (vf). CβP polymerization is complete (arrow) and the barbule cells further elongate. Legends: ba, barb cells; v, barb vane ridge cells and cytoplasm; s, supportive cells. The frames (dashed square) on each illustration of barbule stages indicate the approximate location within barbules where the TEM micrographs were obtained. Scale bars in electron micrographs: P1, P2, and P4, 1 μm; and P3, 2 μm.

ramogenic zone (area of the epidermal cylinder where cells start to differentiate into barb ridges; Fig 2A) are thin (~1.3 μm) and tubular, containing a few immature melanosomes concentrated at the distal end (Fig. 2B, P1). In phase 2 (P2), the cells at the apex of a barbule widen, adopting an ovate shape. These cells start folding, forming a curved flange (the dorsal flange of the barb). Numerous melanosomes with random orientations have reached these barbule cells and fill them in. Feather CβPs starts to polymerize into long filaments and phase separate from the cytoplasm as we see incipient corneous beta-bundles on the lower side of the flange (Fig. 2B, P2). Barbule cells in phase 3 no longer appear round, as cells on both flanges have increased in length and flattened. The corneous beta-bundles are visible on the lower edge of the dorsal barbule cell and cause a longitudinal separation of the barbule's contents wherein melanosomes are limited to the upper side of the barbule flange and the dense corneous beta-bundles are concentrated on the lower side. Melanosomes in this barbule phase show a moderate degree of orientation in parallel layers, particularly towards the periphery (Fig 2B, P3). In phase 4, barbules have attained their boomerang shape as cells on both flanges further elongate. Cornification of feather CβP within the barbule has progressed and now the entire reverse side of the barbules is electron dense, indicating that corneous beta-bundles are absent. The majority of melanosomes present in cells of the dorsal flange are now organized into parallel layers. Small melanosomes present in cells of the ventral flange of the barbule are aligned in the periphery (Fig 2B, P4).

Melanosome morphology

We did not observe melanosomes that had not yet begun to synthesize melanin (i.e., pre-melanosomes) or melanosomes with scaffold of protein fibrils (corresponding to maturation stages I and II identified by Raposo and Marks 2007). The earliest melanosomes we observed likely correspond to maturation stage III (characterized by the start of melanin synthesis; Raposo and Marks 2007) and were located inside melanocytes in the feather pulp and lower bulge of the developing feather (Figs. 2A and 3A). These melanosomes have a cylindrical shape and contain on average 10 internal holes or vesicles. They are lightly pigmented and in some cases t the pigment accumulates around the

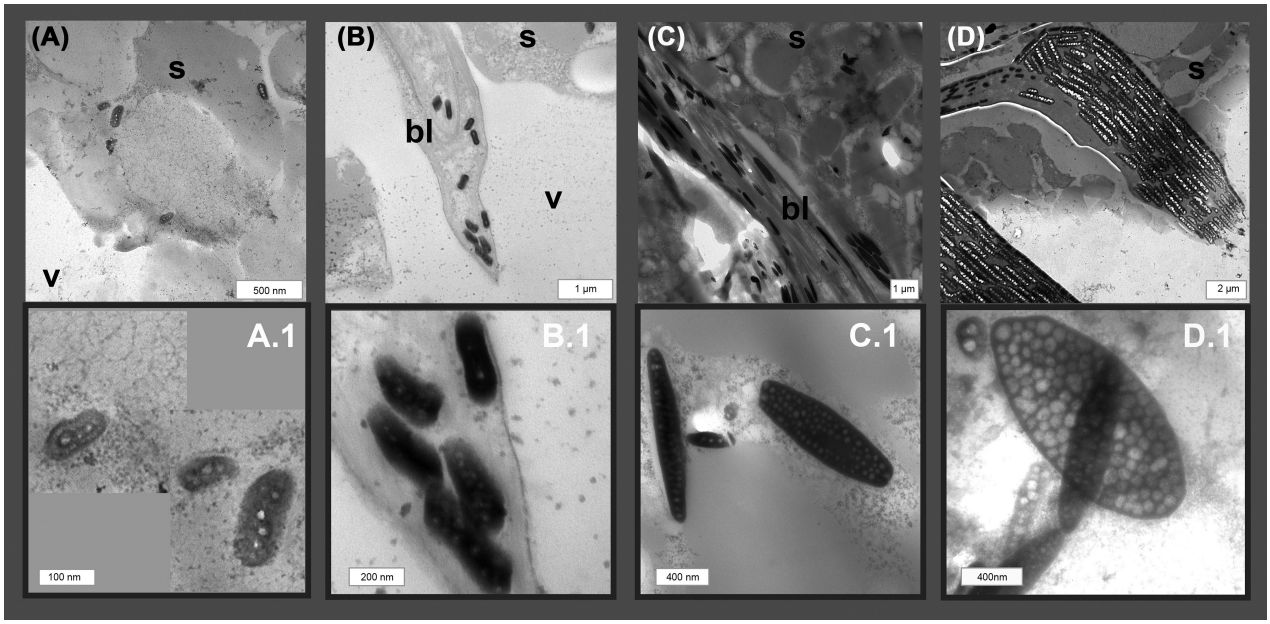

Fig. 3 Developmental sequence of hummingbird melanosomes. (**A**) Earliest melanosomes observed inside melanocytes within the feather pulp and lower bulge of the ramogenic zone. Close-up view A.1 shows several vesicles inside melanosomes. (**B**) Later inside basal barbule cells (stage P1, Fig. 1), melanosomes are still tubular but appear heavily melanized (B.1), then in (**C**), melanosomes seen in transport to keratinocytes seem to elongate and flatten (C.1) inside cells of the ventral flange of barbules (in stage P3). (**D**) Mature melanosomes inside barbules (stage P4) align in parallel layers within the barbule and display an elliptical shape (D.1). Internal vesicles fill the entire melanosome. Scale bars: A: 500 nm, B and C: 1 µm, D: 2 µm. Closeups: A.1: 100 nm, B.1: 200 nm, C.1 and D.1: 400 nm. Legends: bl, barbule cells; s, supportive cells; v barb vane ridge occupied by cytoplasm and supportive cells.

vesicles (Fig. 3A.1). In phase two, melanosomes are transported to keratinocytes via melanocyte extensions and both melanin synthesis and melanosome size increase (Table 1; Fig. 3B).

It is during transport to the ventral flange of barbules that most melanosomes elongate drastically (Table 1) and adopt a flattened, oval shape by widening their *Y*-axis (Figs. 1C and 3C.1). In this phase (P3), melanosome geometry is largely anisotropic. These melanosomes also display large numbers of internal vesicles (mean count = 80 vesicles) and become oriented parallel to the plane of the cut (Fig. 3D). When melanosomes reach the dorsal flange of barbules they appear mature and have doubled in size (Table 1). We see fully enlarged melanosomes only on the dorsal flange of the barbule. The internal vesicles have tripled in size (Table 1) and fill up ~80% of the melanosome volume (mean count = 125 vesicles). The vesicles converge at junctions with average angles of 122 ± 3° creating a pattern resembling typical dry foam systems (Supplementary Fig. S1). The size of melanosomes in the periphery of barbules does not increase and they retain the morphology of those seen in the ventral flange of the barbule. Inside the dorsal flange of mature barbules (phase 4), aligned melanosomes show a gradient in size, becoming slightly larger from the upper to the lower edge of the barbule cell (Fig. 4).

Discussion

We hypothesized that melanosome organization into aligned layers within barbule cells occurs passively through self-assembly. We observed that melanosome alignment temporally coincides with barbule elongation and feather CβP stabilization. Cornification of CβP within barbule cells indicates a decrease in cellular metabolism associated with cell death (Alibardi 2006), which was reflected by the formation of dense filament-matrix structures. Thus, as observed in previous studies (Maia et al. 2012), the formation of organized layers of melanosomes and CβP spacing between them likely occurs through passive self-assembly processes after cellular metabolism has ceased.

In hummingbird barbules, as in iridescent blue-black grassquit barbules (Maia et al. 2012), depletion-attraction forces could drive melanosomes towards the barbule edge and contribute to their alignment. This self-organization may be predicted by the Asakura–Oosawa model of attraction forces resulting from osmotic depletion (Yodh et al. 2001). In mixtures of hard ("noninteracting") particles and polymers (in this case, melanosomes and feather CβP), the central polymer mass cannot occupy a region closer than its own radius on the surface of the particle, creating an area of excluded volume surrounding the particle. As the large

Table 1 Change in morphology of melanosomes in developing hummingbird barbules. Phases and locations of melanosomes are represented in Fig. 3. Measured dimensions of melanosomes correspond to those shown in Fig. 1 and are given in nm. Average (± standard error of the mean) is provided

Phase–location (*N* = melanosomes measured)	Melanosome			Vesicle diameter
	Length	Width	Thickness[a]	
1. Lower bulge (25)	260 (20)	120 (8)	—	30 (2)
2. Melanocyte extensions (50)	350 (18)	140 (6)	—	32 (1)
3. Barbule ventral flange (55)	1150 (250)	340 (7)	130 (5)	32 (3)
4. Barbule periphery (50)	561 (53)	142 (8)	—	34 (1)
5. Dorsal flange of barbules (70)	2020 (120)	1300 (30)	330 (7)	124 (3)

[a]Melanosome thickness is only perceivable and quantifiable after the organelle has adopted a flattened shape in phase 3.

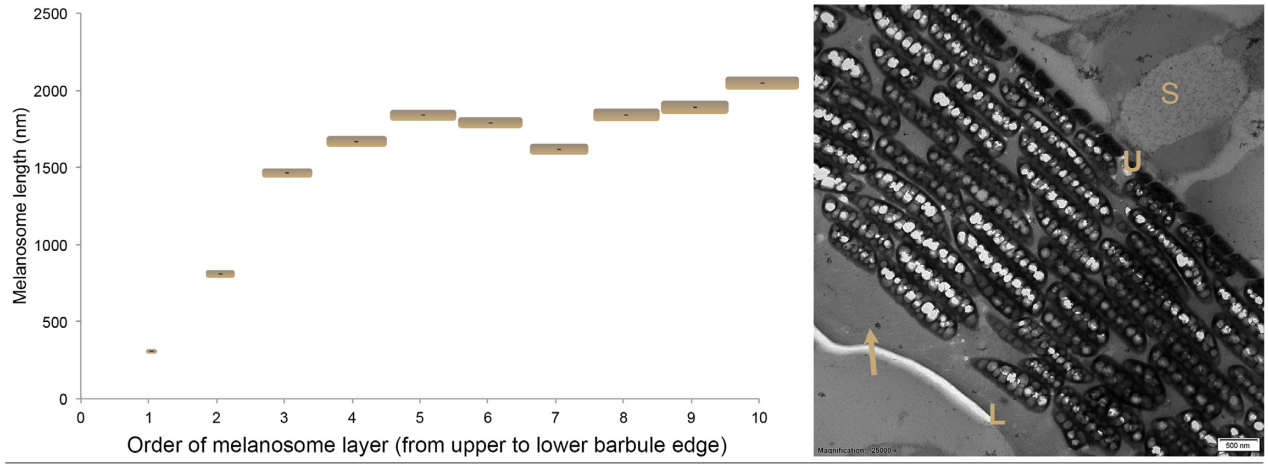

Fig. 4 Mature melanosome size in relation to the location within the barbule cell (order of melanosome layer from the upper side (U) of the barbule cell to the lower side (L) of the cell). Electron micrograph shows a cross-section of a barbule cell (of dorsal flange), where aligned layers of melanosomes are located. Small melanosomes are distributed along the periphery and mature melanosomes in aligned layers progressively increase in length and thickness. Lower edge of the barbule cell appears solid and fully cornified (arrow). S, supporting cell.

particles approach one another, these areas of excluded volume overlap, resulting in a larger volume that can be occupied by the polymer and therefore an increase in entropy reducing free energy. This overlap leads to the depletion of the polymer in the gaps between particles, creating an osmotic gradient that attracts particles to one another. This model suggests that the production of complex, nanostructured iridescent feathers can be less or equally energetically expensive than the production of typical unorganized melanin-based plumage because it relies on passive self-assembly forces, requiring only a small increase in energy to produce more feather CβP and melanin. In addition, the large size and concentration of platelets within hummingbird barbules would increase the excluded volume overlap between particles (Kaplan et al. 1994) and should result in the depletion of CβP in the gaps between melanosomes, increasing the attraction between them and leading to a prominent and consistent melanosome layer formation.

Changes in melanosome morphology and self-assembly of multilayered photonic structures are correlated to barbule maturation. First, the polymerization of CβP was dominant on the lower side of the flanges, effectively creating a division between the upper and lower sides of the flanges and decreasing the area available for dispersion of melanosomes within the barbules by roughly one-third.

Surface tension within barbule cells (i.e., the energy present at the interface between the cell membrane and the cytoplasm inside cells; Clark and Paluch 2011) may also affect self-assembly of hummingbird melanosomes. As in most iridescent species, barbules of *C. anna* are elliptical and flat. Hydrostatic pressure and surface tension inside cells increase with ellipticity, as cell boundaries are governed by Laplace's law linking internal pressure, tension and curvature (Fisher-Friedrich et al. 2014). An increase in the ordering of anisotropic particles is observed when surface tension is high (Dugyala and Basavaraj 2015) because a large capillary flow in-

creases the pinning of particles to the contact line, resulting in the aggregation of particles at the periphery (Still et al. 2012). An intriguing possibility is that barbule flattening and its effects on internal surface tension lead directly to melanosome self-assembly.

This distinctive barbule shape is achieved first by a clear asymmetry in the growth of dorsal and ventral flanges of barbules. From the earliest phase, cells on the dorsal flange grow more than those on the ventral flange, ballooning into a round volume into which melanosomes are transferred. These apical cells then fold, effectively forming a boomerang shape. This asymmetry also means that during development, processes occur in isolation within cells of the two flanges. Once barbule plates form at the base of the ramogenic zone, barbule growth occurs only through cell enlargement (not by the addition of new cells; Lillie and Juhn 1932; Lucas and Stettenheim 1972) via CβP accumulation within barbule cells and the mechanical pressures exerted on them by the sheath (Lucas and Stettenheim 1972). Consequently, the asymmetric growth between the flanges could reflect an increased production of CβP in the dorsal (cell) flange relative to cells in the ventral side and/or anisotropic friction experienced by the two sides as a result of their differential orientation relative to the plane of growth (e.g., perpendicular in dorsal vs. parallel in ventral flanges).

Morphogenesis of melanosome vesicles

How are air-filled vesicles (distinct from the vast majority of avian melanosomes that are solid) within hummingbird melanosomes formed? They increased in size and number as melanosomes matured but were observed at all developmental stages. Their early presence suggests that they are intraluminal vesicles (ILVs), typical of multivesicular bodies (MVBs) and pre-melanosomes (Hurbain et al. 2008). Similar vesicles are present during development of fish melanosomes (Turner et al. 1975; Burgoyne et al. 2015) and may serve as scaffolds for melanin deposition in place of protein fibrils (Turner et al. 1975). Vesicles form by inward budding of the organelle membrane into the lumen of MVBs and pre-melanosomes and may contain certain combinations of lipids, proteins and signaling molecules (Ludwig and Giebel 2012). Exclusively in melanosomes, ILVs seed the formation of protein (PMEL) fibrils, which in turn guide melanin deposition (Hurbain et al. 2008). This could explain why we observed denser melanin-containing areas around the vesicles in early melanosomes. In addition, ILVs typically decrease in size and number as melanosomes elongate (Hurbain et al. 2008), consistent with their absence in most bird species. However, the presence of transmembrane proteins (e.g., tetraspanin CD36) on ILV's and their association with PMEL might help retain these vesicles throughout melanosome development in hummingbirds by preventing their migration and degradation. Alternatively, ILVs could actually be present in melanosomes of other species but not visible because they are densely covered by melanin (Van Niel 2016).

We found that during maturation, hummingbird melanosomes grow roughly 10 times in size, becoming clearly elliptical. Their final size is determined by the amount of melanin produced by the melanosome (i.e., its metabolic activity; Marshall 2012) and could also be affected by the amount of vesicles inside them. The latter indeed increase at least three times in size during melanosome maturation. The morphology of vesicles in mature melanosomes and their contact angles with the melanin matrix bear some similarity to bubbles in dry, polyhedral foams (Supplementary Fig. S1). Moreover, the expansion of vesicles could arise from a dynamic foaming process within the developing organelles. Foaming occurs when gas is dispersed in a continuous liquid phase (colloidal dispersion; Schramm 2006). Rheological studies of foams show that air vesicles within a colloidal mix are expected to grow following a decrease in pressure within the containing membrane (Schramm 2006). If we consider the melanosome contents a colloidal suspension (Wolbarsht et al. 1981), an appealing hypothesis is that analogous processes could produce the characteristic porous morphology of hummingbird platelets.

How materials become organized into optically active nanostructures in developing biological materials is of both fundamental and applied interest. We found no evidence that producing iridescent barbules requires more energy expenditure than typical barbules, as neither the production of hollow platelet-shaped melanosomes nor their organization into multilayers is guided by active cellular processes. Rather, a few shifts in the typical pattern of feather development are sufficient. First, melanosomes contain holes at their initial formation, becoming more porous after they transfer to keratinocytes. Anisotropic growth of melanosomes following transfer leads to their distinctive platelet shape. Second, organization into multilayers is driven by preferential growth of one side of the barbule, which shrinks available space for melanosomes and drives their arrangement into low-energy, densely packed configuration. Both of these patterns are broadly supported by gene expression data from developing iridescent superb starling (*Lamprotornis superbus*) feathers (Rubenstein et al. 2021), which suggest that, while iridescent feathers are less costly to grow than noniridescent feathers, they require greater expression of genes related to cell organization. These latter genes may be linked to observed

differences in melanosome and barbule morphology both in starlings and hummingbirds, but more detailed studies are needed. Verifying these hypothesized mechanisms and identifying their molecular, physical, and cellular bases will be fascinating objectives of future research, and possibly inspiring for new colored material manufacturing methods.

Supplementary data

Supplementary data available at *ICB* online.

Acknowledgments

We sincerely thank Jérôme Casas, Florent Figon, and Leila Deravi for the invitation to present this study as part of a special symposium on the integrative biology of pigment organelles and for their patience in waiting for its submission. We are grateful to Prof. Ali Dhinojwala for invaluable discussions about foaming processes.

Funding

This work was supported by a MURI through the Air Force Office of Scientific Research [FA9550-18-0477]; FWO [G007117N] and HFSP [RGP 0047].

Data availability

All data are incorporated into the article and its online supplementary material. Electron micrographs used in this article will be shared on reasonable request to the corresponding author.

References

Alibardi L. 2006. Cells of embryonic and regenerating germinal layers within barb ridges: implication for the development, evolution and diversification of feathers. J Submicrosc Cytol Pathol 38:51.

Alibardi L. 2007. Keratinization of sheath and calamus cells in developing and regenerating feathers. Ann Anat 189:583–95.

Alibardi L. 2016. The process of cornification evolved from the initial keratinization in the epidermis and epidermal derivatives of vertebrates: a new synthesis and the case of sauropsids. Int Rev Cell Mol Biol 327:263–319.

Burgoyne T, O'Connor MN, Seabra MC, Cutler DF, Futter CE. 2015. Regulation of melanosome number, shape and movement in the zebrafish retinal pigment epithelium by OA1 and PMEL. J Cell Sci 128:1400–7.

Clark AG, Paluch E. 2011. Mechanics and Regulation of Cell Shape During the Cell Cycle. In: J. Kubiak, editors. Cell Cycle in Development. Results and Problems in Cell Differentiation, Springer. p. 31–73. https://doi.org/10.1007/978-3-642-19065-0_3.

Cott HB, Huxley J. 1940. Adaptive coloration in animals. Methuen: Oxford University Press. p. 508

D'Alba L, Wang B, Vanthournout B, Shawkey MD. 2019. The golden age of arthropods: ancient mechanisms of colour production in body scales. J R Soc, Interface 16:20190366.

Dufresne ER, Noh H, Saranathan V, Mochrie SGJ, Cao H, Prum RO. 2009. Self-assembly of amorphous biophotonic nanostructures by phase separation. Soft Matter 5: 1792–5.

Dugyala VR, Basavaraj MG. 2015. Evaporation of sessile drops containing colloidal rods: coffee-ring and order–disorder transition. J Phys Chem B 119:3860–7.

Durrer H. 1986. Colouration. In Biology of the integument. Springer Berlin: Heidelberg. p. 239–47.

Durrer H, Villiger W. 1967. Bildung der Schillerstruktur beim Glanzstar. Z Zellforsch 81:445–56.

Eliason CM, Bitton P-P, Shawkey MD. 2013. How hollow melanosomes affect iridescent colour production in birds. Proc R Soc B: Biol Sci 280:20131505.

Eliason CM, Maia R, Parra JL, Shawkey MD. 2020. Signal evolution and morphological complexity in hummingbirds (Aves: Trochilidae). Evolution 74:447–58.

Fischer-Friedrich E, Hyman AA, Jülicher F, Müller DJ, Helenius J. 2014. Quantification of surface tension and internal pressure generated by single mitotic cells. Sci Rep 4:6213.

Foth C, 2020. Introduction to the morphology, development, and ecology of feathers. In: The evolution of feathers. Cham: Springer. p. 1–11.

Giraldo MA, Parra JL, Stavenga DG. 2018. Iridescent colouration of male Anna's hummingbird (*Calypte anna*) caused by multilayered barbules. J Comp Physiol A 204:965–75.

Greenewalt CH, Brandt W, Friel DD. 1960. Iridescent colors of hummingbird feathers. J Opt Soc Am 50:1005–13.

Hill GE, McGraw KJ. 2006. Bird coloration: mechanisms and measurements. Harvard University Press: Cambridge, MA.

Hurbain I, Geerts WJC, Boudier T, Marco S, Verkleij AJ, Marks MS, Raposo G. 2008. Electron tomography of early melanosomes: implications for melanogenesis and the generation of fibrillar amyloid sheets. Proc Natl Acad Sci 105:19726–31.

Kaplan PD, Rouke JL, Yodh AG, Pine DJ. 1994. Entropically driven surface phase separation in binary colloidal mixtures. Phys Rev Lett 72:582–5.

Lillie FR, Juhn M. 1932. The physiology of development of feathers. I. Growth-rate and pattern in the individual feather. Physiol Zool 5:124–84.

Lucas AM, Stettenheim PR. 1972. Avian anatomy: integument U.S. agricultural research service. U.S. Agricultural Research Service: Washington D.C.

Ludwig A-K, Giebel B. 2012. Exosomes: small vesicles participating in intercellular communication. Int J Biochem Cell Biol 44:11–5.

Maia R, Macedo RHF, Shawkey MD. 2012. Nanostructural self-assembly of iridescent feather barbules through depletion attraction of melanosomes during keratinization. J R Soc, Interface 9:734–43.

Maia R, Rubenstein DR, Shawkey MD. 2013. Key ornamental innovations facilitate diversification in an avian radiation. Proc Natl Acad Sci 110:10687–92.

Marshall WF. 2012. Organelle size control systems: from cell geometry to organelle-directed medicine. Bioessays 34: 721–4.

Meadows MG, Roudybush TE, McGraw KJ. 2012. Dietary protein level affects iridescent coloration in Anna's hummingbirds, *Calypte anna*. J Exp Biol 215:2742–50.

Onelli OD, van de Kamp T, Skepper JN, Powell J, Rolo T dos S, Baumbach T, Vignolini S. 2017. Development of structural colour in leaf beetles. Sci Rep 7:1373.

Parker AR, Townley HE. 2007. Biomimetics of photonic nanostructures. Nat Nanotechnol 2:347–53.

Prum RO, Dufresne ER, Quinn T, Waters K. 2009. Development of colour-producing β-keratin nanostructures in avian feather barbs. J R Soc, Interface 6:S253–65.

Prum RO. 1999. Development and evolutionary origin of feathers. J Exp Zool 285:291–306.

Prum RO. 2006. Anatomy, physics, and evolution of avian structural colors. In: Hill GE, McGraw KJ, editors. Bird coloration, Volume 1: Mechanisms and measurements. Cambridge, MA: Harvard University Press. p. 295–353.

Raposo G, Marks MS. 2007. Melanosomes—dark organelles enlighten endosomal membrane transport. Nat Rev Mol Cell Biol 8:786–97.

Rubenstein DR, Corvelo A, MacManes MD, Maia R, Rousaki A, Vandenabeele P, Shawkey MD, Solomon J. 2021. Feather gene expression elucidates the developmental basis of plumage iridescence in African starlings. J Hered https://doi.org/10.1093/jhered/esab014. esab014.

Schramm LL. 2006. Emulsions, foams, and suspensions: fundamentals and applications. John Wiley & Sons: Weinheim, Germany.

Shawkey MD, D'Alba L, Xiao M, Schutte M, Buchholz R. 2015. Ontogeny of an iridescent nanostructure composed of hollow melanosomes. J Morphol 276:378–84.

Srinivasarao M. 1999. Nano-optics in the biological world: beetles, butterflies, birds, and moths. Chem Rev 99:1935–62.

Still T, Yunker PJ, Yodh AG. 2012. Surfactant-induced marangoni eddies alter the coffee-rings of evaporating colloidal drops. Langmuir 28:4984–8.

Turner WA, Taylor JD, Tchen TT. 1975. Melanosome formation in the goldfish: the role of multivesicular bodies. J Ultrastruct Res 51:16–31.

van Niel G. 2016. Study of exosomes shed new light on physiology of amyloidogenesis. Cell Mol Neurobiol 36:327–42.

Watterson RL. 1942. The morphogenesis of down feathers with special reference to the developmental history of melanophores. Physiol Zool 15:234–65.

Wolbarsht ML, Walsh AW, George G. 1981. Melanin, a unique biological absorber. Appl Opt 20:2184–6.

Xiao M, Shawkey MD, Dhinojwala A. 2020. Bioinspired melanin-based optically active materials. Adv Opt Mater 8:2000932.

Yodh AG, Lin K, Crocker JC, Dinsmore AD, Verma R, Kaplan PD. 2001. Entropically driven self-assembly and interaction in suspension. Phil Trans R Soc A: Math Phys Eng Sci 359:921–37.